Classical theory of cylindrical nonlinear optics: Second-harmonic generation

Hao Xiong,[1,*] Liu-Gang Si,[1,†] Jun Feng Guo,[1] Xin-You Lü,[2] and Xiaoxue Yang[1]

[1]*Wuhan National Laboratory for Optoelectronics and School of Physics, Huazhong University of Science and Technology, Wuhan 430074, People's Republic of China*

[2]*School of Physics, Ludong University, Yantai 264025, People's Republic of China*

(Received 16 December 2010; published 29 June 2011)

The second-harmonic generation of cylindrical electromagnetic waves in a nonlinear nondispersive medium is investigated two separate ways. One method uses the exact solutions of the Maxwell equations, which describe propagation of cylindrical electromagnetic waves, and the other method uses the traditional coupled-wave equations, which are derived from the interaction between cylindrical electromagnetic waves and a nonlinear nondispersive medium. The results obtained by these two methods are concordant with each other. We also show that both methods are useful in dealing with the problem of cylindrical second-harmonic generation and each of them has particular advantages in several aspects. The method of using the exact solution can solve problems of second-harmonic generation under initial-value and boundary-value conditions and the approach of using coupled-wave equations can be directly extended to describe other nonlinear phenomena such as sum-frequency and four-wave mixing.

DOI: 10.1103/PhysRevA.83.063845 PACS number(s): 42.65.Ky, 03.50.De, 41.20.Jb

I. INTRODUCTION

Electromagnetic wave propagation in nonlinear media is a fundamental problem in physics and many interesting electromagnetic phenomena occur when the dielectric susceptibility of a medium is a nonlinear function of the electric-field amplitude [1–7]. One such electromagnetic phenomenon is optical second-harmonic generation (SHG), which was initially observed in quartz [3]. Since then a number of important features of SHG have been found and SHG has become one of the most intensively studied effects in nonlinear optics [6–19]. For example, it has been widely used as a noninvasive, noncontact probe of electronic and structural properties of crystals [7]. A phenomenological approach to describing nonlinear optics phenomena (including SHG) was developed in the 1960s [4–7]. Most works on the subject of nonlinear optics, including SHG, consider plane nonlinear waves. The process of SHG is shown in Fig. 1(a). The features of nonlinear optics with cylindrical or spherical waves (so-called cylindrical or spherical nonlinear optics), however, remain poorly studied [1,2]. Figure 1(b) shows a schematic diagram of cylindrical harmonic generation. In this paper we study SHG in cylindrical nonlinear optics, which are different from the plane nonlinear optics phenomena.

In this article we employ two different methods to investigate SHG of cylindrical electromagnetic waves in a nonlinear nondispersive medium. First, following the method proposed in Ref. [1] for constructing exact axisymmetric solutions of the Maxwell equations in a nonlinear nondispersive medium, we demonstrate that this exact axisymmetric solution, which has been successfully used to discuss electromagnetic shock waves [1], can also be used to describe the SHG of cylindrical electromagnetic waves. Furthermore, this exact solution method has particular advantages in several aspects. Our study may be used in nonlinear resonators, nanoscale optical element, and optical regulation [1,6,7]. Second, we imitate plane nonlinear optics to derive coupled-wave equations, which describe the interaction between cylindrical electromagnetic waves and a nonlinear medium, to study the SHG of cylindrical electromagnetic waves (discussed in detail in Sec. III).

The outline of the paper is as follows. In Sec. II we use exact solutions to investigate cylindrical SHG and show that second-harmonic generation results quite naturally from exact solutions. We also use an effective approximation to simplify the exact solution and show that the method of using exact solutions can solve problems of second-harmonic generation under boundary-value conditions. In Sec. III we derive coupled-wave equations to investigate the SHG of cylindrical electromagnetic waves and compare the results with the results obtained using the exact solution. We also discuss the phase-matching condition of SHG in cylindrical nonlinear optics in Sec. III. In Sec. IV we briefly discuss the differences between our system and conical wave propagation; a possible experimental setup is also shown schematically. Our conclusions are summarized in Sec. V.

II. ANALYSIS OF SECOND-HARMONIC GENERATION BY USING THE EXACT SOLUTION

A. Cylindrical wave propagation in an infinite medium

We considering a medium that possesses an axis of symmetry [shown in Fig. 1(b)] that is taken as the z axis of a cylindrical coordinate system (r,ϕ,z) and use the axisymmetric model in which the fields are independent of ϕ and z to write the Maxwell equations as [1]

$$\frac{\partial H}{\partial r}+\frac{H}{r}=\varepsilon(E)\frac{\partial E}{\partial t},\quad \frac{\partial E}{\partial r}=\mu_0\frac{\partial H}{\partial t}, \tag{1}$$

where $H\equiv H_\phi(r,t)$, $E\equiv E_z(r,t)$, and $\varepsilon(E)=dD/dE=\epsilon_0\varepsilon_1\exp(\alpha E)$, with ε_1 and α known constants. Thus

*haoxiong1217@gmail.com
†siliugang@gmail.com

 ©2011 American Physical Society

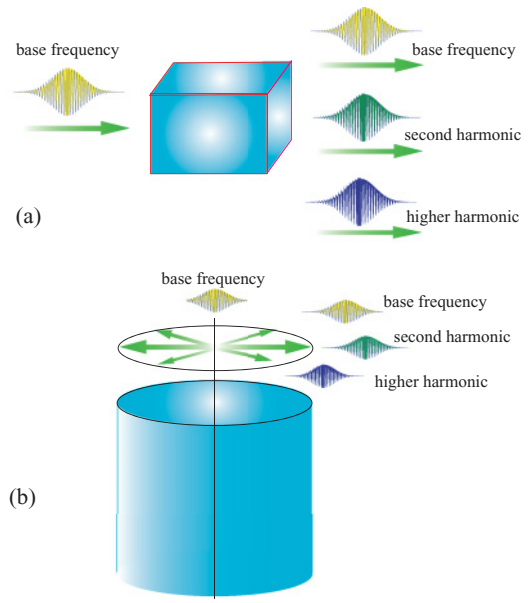

FIG. 1. (Color online) (a) Schematic diagram of conventional plane nonlinear optics. When a beam of light with base frequency is incident upon a nonlinear medium, second- and higher-harmonic generation occur. (b) Schematic diagram of cylindrical nonlinear optics. The light source is placed on the axis of a nonlinear medium and cylindrical electromagnetic waves are emitted. Second- and higher-harmonic generation occur also when the cylindrical electromagnetic waves with base frequency propagate in the nonlinear medium; however, such harmonic generations are different from plane harmonic generations.

$P = D_0 + \epsilon_0(\varepsilon_1 - 1)E + \epsilon_0\varepsilon_1\alpha E^2/2 + \cdots$ and $\chi^{(2)} = \varepsilon_1\alpha/2$. The exact solution of such a system can be written as [1]

$$E = \mathcal{E}\left(\rho e^{\alpha E/2}, \tau + \frac{Z_0\alpha\rho H}{2\sqrt{\varepsilon_1}}\right),$$
$$H = \frac{\sqrt{\varepsilon_1}e^{\alpha E/2}}{Z_0}\mathcal{H}\left(\rho e^{\alpha E/2}, \tau + \frac{Z_0\alpha\rho H}{2\sqrt{\varepsilon_1}}\right), \qquad (2)$$

where $\mathcal{E}(\rho,\tau)$ and $\mathcal{H}(\rho,\tau)$ represent the solution of the linear problem in Eq. (1) with $\alpha = 0$, $\rho = r/a$, $\tau = t/\sqrt{\epsilon_0\varepsilon_1\mu_0}a$, and $Z_0 = \sqrt{\mu_0/\epsilon_0}$, with a a constant with the dimension of length.

We begin our discussion by considering cylindrical wave propagation in an infinite medium. The solution of the linear problem is $\mathcal{E}(r,t) = \zeta J_0(kr)\cos(\varpi t)$ and $\mathcal{H}(r,t) = -\zeta J_1(kr)\sin(\varpi t)$, which when rewritten in terms of the variable (ρ,τ) becomes $\mathcal{E}(\rho,\tau) = \zeta J_0(k\rho a)\cos(\varpi\tau\sqrt{\epsilon_0\varepsilon_1\mu_0}a)$ and $\mathcal{H}(\rho,\tau) = -\zeta J_1(k\rho a)\sin(\varpi\tau\sqrt{\epsilon_0\varepsilon_1\mu_0}a)$. From Eq. (2) we can obtain the solution of the nonlinear problem:

$$E = \zeta J_0(kre^{\alpha E/2})\cos(\varpi t + \alpha\mu_0\varpi rH/2),$$
$$H = -\zeta\frac{\sqrt{\varepsilon_1}e^{\alpha E/2}}{Z_0}J_1(kre^{\alpha E/2})\sin(\varpi t + \alpha\mu_0\varpi rH/2). \qquad (3)$$

Here J_m is a Bessel function of the first kind of order m, ζ is a constant, and $k = \varpi\sqrt{\epsilon_0\varepsilon_1\mu_0}$. The solution shows that the electric field and magnetic field of the cylindrical electromagnetic wave in a nonlinear medium are not separate but coupled with each other. For simplicity we consider that H can be approximately written as $H \approx \gamma\sin(\varpi t)$ at a certain r, where $\gamma = -\zeta\sqrt{\varepsilon_1}J_1(kr)/Z_0$; then we can obtain $E \propto \cos[\varpi t + \gamma\alpha\mu_0\varpi r\sin(\varpi t)/2] = \cos(\varpi t)\cos[\gamma\alpha\mu_0\varpi r\sin(\varpi t)/2] - \sin[\gamma\alpha\mu_0\varpi r\sin(\varpi t)/2]\sin(\varpi t)$. If α is small enough, ensuring that $\alpha\mu_0\varpi rH \ll 1$, then $\cos[\gamma\alpha\mu_0\varpi r\sin(\varpi t)/2] \approx 1$ and $\sin[\gamma\alpha\mu_0\varpi r\sin(\varpi t)/2] \approx \gamma\alpha\mu_0\varpi r\sin(\varpi t)/2$, so we can obtain $E \propto \cos(\varpi t) - \gamma\alpha\mu_0\varpi r\sin^2(\varpi t)/2 = \cos(\varpi t) + \gamma\alpha\mu_0\varpi r\cos(2\varpi t)/4 - \gamma\alpha\mu_0\varpi r/4$. The term $-\gamma\alpha\mu_0\varpi r/4$ in the expression reflects optical rectification or the photogalvanic effect. The term $\gamma\alpha\mu_0\varpi r\cos(2\varpi t)/4$ implies that the second harmonic results quite naturally from the exact solution in Eq. (3). α, ϖ, r, and the magnetic-field amplitude γ will influence the SHG characterization of the cylindrical electromagnetic wave. By defining η_T as the ratio of the amplitude of the second harmonic to that of the base frequency in the frequency spectrogram, we have $\eta_T = |\gamma|\alpha\mu_0\varpi r/4 = |\zeta\alpha krJ_1(kr)|/4$. For the case of α not being small enough, by using $\sin\theta \approx \theta - \theta^3/6$ and $\cos\theta \approx 1 - \theta^2/2$, we can find the third and higher harmonics. In fact, the approximation of $H \propto \sin(\varpi t)$ is sufficiently effective, but not necessary. One can use a high-order approximation, for example, $H \approx \gamma\sin[\varpi t + \gamma\alpha\mu_0\varpi r\sin(\varpi t)]$, which also leads to the third and higher harmonics. Using the formula $\eta_T = |\zeta\alpha krJ_1(kr)|/4$, we can find the extreme value of η_T. We give an example in the following.

Figure 2 shows the results of the calculation of the exact solution of Eq. (3). By using $\alpha = 0.14$, $\varpi = 6\times10^8$ MHz, $\zeta = 1$, and $\varepsilon_1 = 2$, Fig. 2(a) shows the frequency spectrum

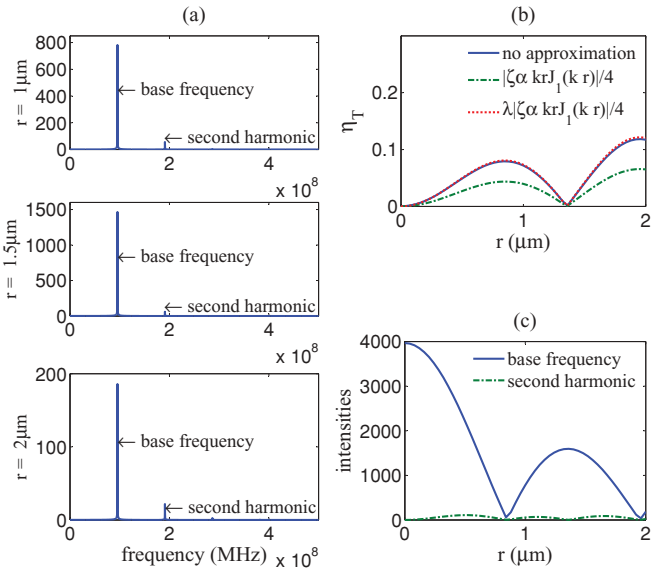

FIG. 2. (Color online) Results of cylindrical wave propagation in an infinite medium calculated using the exact solution of Eq. (3). (a) Frequency spectrum of the electric field at various r. We use $\alpha = 0.14$, $\varpi = 6\times10^8$ MHz, $\zeta = 1$, and $\varepsilon_1 = 2$. (b) Efficiencies of SHG η_T with different r, which ranges from 0 to 2 μm. The blue solid curve represents the results calculated directly using the exact solution of Eq. (3), the red dotted curve represents the results of calculations using $\eta_T = \lambda|\zeta\alpha krJ_1(kr)|/4$, and the green dashed curve represents the results of calculations using $\eta_T = |\zeta\alpha krJ_1(kr)|/4$. (c) Results of the variation of the intensities with r of the two frequency components calculated using the exact solution of Eq. (3).

of the electric field at various r. There is an obvious second harmonic in the frequency spectrum. It can be found that the amplitude of the second harmonic does not increase with r. In Fig. 2(a) the amplitude of the second harmonic at $r = 1.5\ \mu$m is the smallest one. Figure 2(b) shows the curve of η_T as a function of r calculated by different methods. The blue solid curve represents the results calculated directly using the exact solution of Eq. (3); the green dashed curve represents results calculated using $\eta_T = |\zeta\alpha kr J_1(kr)|/4$, which fit well with the results calculated directly using the exact solution of Eq. (3). The difference between the two curves arises from the approximation of $e^{\alpha E/2} \approx 1$. To describe η_T more precisely, we introduce a correction factor $\lambda \approx 1.86$. Figure 2(b) shows that $\eta_T = \lambda|\zeta\alpha kr J_1(kr)|/4$ (the red dot curve) fits precisely with the results calculated directly using the exact solution of Eq. (3). The results of the variation of the intensities with r of the two frequency components calculated using the exact solution of Eq. (3) are shown in Fig. 2(c).

B. Advanced approximation and origin of the correction factor

As an approximate solution $E = \zeta J_0(kr)\cos(\varpi t) + \zeta J_0(kr)\gamma\alpha\mu_0\varpi r\cos(2\varpi t)/4 - \gamma\alpha\mu_0\varpi r/4$ shows most of the nonlinear optical phenomena; however, it still need to be improved. By using numerical simulation we verify that $H \approx \gamma\sin(\varpi t)$ is a good approximation and the errors mainly arise from the approximation $\exp(\alpha E/2) \approx 1$, precisely, $J_0(kre^{\alpha E/2}) \approx J_0(kr)$. In what follows we propose an improved approximation to replace the approximation $J_0(kre^{\alpha E/2}) \approx J_0(kr)$. As mentioned in Sec. II A, a correction factor $\lambda \approx 1.86$ is introduced by numerical simulation to describe second-harmonic generation more precisely. Here we will show why this correction factor is introduced.

We introduce a function $f(x,b)$ as

$$J_0(xb) = J_0(x)f(x,b) \tag{4}$$

such that $f(x,1) = 1$ and

$$f(x,1+\Delta) \approx f(x,1) + f'(x,1)\Delta, \tag{5}$$

where $|\Delta| \ll 1$ and $f'(x,1) = (\partial f/\partial b)_{b=1} = -xJ_1(x)/J_0(x)$. Thus we obtain

$$f(x,1+\Delta) \approx 1 - \Delta x J_1(x)/J_0(x). \tag{6}$$

Using Eqs. (4) and (6) we can give an approximation of $J_0(kre^{\alpha E/2})$. Following Eq. (4) and considering $|\alpha E| \ll 1$ we write $J_0(kre^{\alpha E/2})$ as

$$\begin{aligned} J_0(kre^{\alpha E/2}) &= J_0(kr)f\left(kr, e^{\alpha E/2}\right) \\ &\approx J_0(kr)f(kr, 1+\alpha E/2). \end{aligned} \tag{7}$$

Using Eq. (6) we obtain

$$J_0(kre^{\alpha E/2}) \approx J_0(kr)\left(1 - \frac{\alpha E kr J_1(kr)}{2J_0(kr)}\right). \tag{8}$$

Now we use Eq. (8) and $H \approx \gamma\sin\varpi t$ to discuss second-harmonic generation. Substituting Eq. (8) into $E = \zeta J_0(kre^{\alpha E/2})\cos(\varpi t + \alpha\mu_0\varpi r H/2)$ we have

$$E \approx \zeta J_0(kr)\left(1 - \frac{\alpha E kr J_1(kr)}{2J_0(kr)}\right)\cos(\varpi t + \Theta\sin\varpi t), \tag{9}$$

where $\Theta = -\alpha\zeta J_1(kr)kr/2$, and Eq. (9) can be write as

$$E \approx E_0 + E_c, \tag{10}$$

where $E_0 = \zeta J_0(kr)\cos(\varpi t + \Theta\sin\varpi t)$ (which has been discussed in detail in Sec. II A) and $E_c = \Theta E\cos(\varpi t + \Theta\sin\varpi t)$ can be considered a correction term of E. There are unknown functions E on each side of Eq. (10). Solving it directly is not recommended. Here we use a simple way of substituting $E = E_0$ into E_c of the right-hand side of Eq. (10) to obtain

$$\begin{aligned} E_c &\approx \Theta\zeta J_0(kr)\cos^2(\varpi t + \Theta\sin\varpi t) \\ &\approx \frac{\Theta}{2}\zeta J_0(kr)(\cos 2\varpi t - 2\Theta\sin\varpi t\sin 2\varpi t + 1). \end{aligned} \tag{11}$$

We find that

$$E_0 \approx \zeta J_0(kr)\left(\cos\varpi t + \frac{\Theta}{2}\cos 2\varpi t - \frac{\Theta}{2}\right), \tag{12}$$

so we can obtain the final result

$$E \approx \zeta J_0(kr)\cos\varpi t + \Theta\zeta J_0(kr)\cos 2\varpi t, \tag{13}$$

where third and higher harmonics are discarded. A comparison of Eqs. (12) and (13) leads to the correction factor $\lambda = 2$, which is in good agreement with the factor introduced in Sec. II A.

C. Cylindrical SHG under boundary-value conditions

We show that using the exact solution in Eq. (3) to study SHG has advantages in several aspects such as problems of SHG under initial-value and boundary-value conditions, which are extremely complicated problems. Here we consider a boundary-value problem with the conditions $\mathcal{E}(1,\tau) = 0$ and the amplitude factor of the wave ζ, which is used in many works [1,2]. The solution of the nonlinear equations [Eqs. (1)] can be written in the form [1]

$$\begin{aligned} E &= \zeta J_0(\kappa_n\rho e^{\alpha E/2})\cos(\kappa_n\theta), \\ H &= -\zeta\frac{\sqrt{\varepsilon_1}e^{\alpha E/2}}{Z_0}J_1(\kappa_n\rho e^{\alpha E/2})\sin(\kappa_n\theta), \end{aligned} \tag{14}$$

where κ_n is the nth root of the equation $J_0(\kappa) = 0$ and $\theta = \tau + Z_0\alpha\rho H/2\sqrt{\varepsilon_1}$. Similarly, we can obtain $E \propto \cos(\kappa_n\tau) - \lambda\kappa_n Z_0\alpha\rho\gamma\sin^2(\kappa_n\tau)/2\sqrt{\varepsilon_1}$. In this case, $\gamma = -\zeta\sqrt{\varepsilon_1}J_1(\kappa_n\rho)/Z_0$ and $\eta_T = \lambda|\zeta\alpha\kappa_n\rho J_1(\kappa_n\rho)|/4$. Using $d\eta_T/d\rho = 0$, we can determine extreme values of η_T, which satisfy $J_0(\kappa_n\rho)\kappa_n\rho = 0$. Obviously, there are two cases: $\kappa_n\rho = 0$ and $J_0(\kappa_n\rho) = 0$. Thus η_T reaches extreme values at $\rho = 0$, $\rho = \kappa_m/\kappa_n$, and $\rho = 1$, where m is an integer that is smaller than n. More specifically, η_T reaches a minimum at $\rho = 0$ and a maximum at $\rho = 1$. With the exceptions $\rho = 0$ and 1, other extreme values satisfy $\kappa_n\rho = \kappa_m$. If we consider fields in the $n = 1$ mode, viz. $\kappa_1 = 2.4048$, we find that η_T increases with ρ. For fields in the $n = 2$ mode, η_T has another extreme value at $\rho = \kappa_1/\kappa_2$; thus η_T has two peaks in the $n = 2$ mode and n peaks in the n mode. The zero points of η_T can be obtained similarly, which satisfy $J_1(\kappa_n\rho)\kappa_n\rho = 0$. There are also two cases: $\kappa_n\rho = 0$ or $J_1(\kappa_n\rho) = 0$. Thus η_T reaches the zero point at $\rho = 0$ and κ_m^1/κ_n, where κ_m^1 is the mth root of the equation $J_1(\kappa) = 0$.

Figure 3 shows the results of calculations of the exact solution in Eq. (14) in the $n = 1$ mode. Similar to Fig. 2(a),

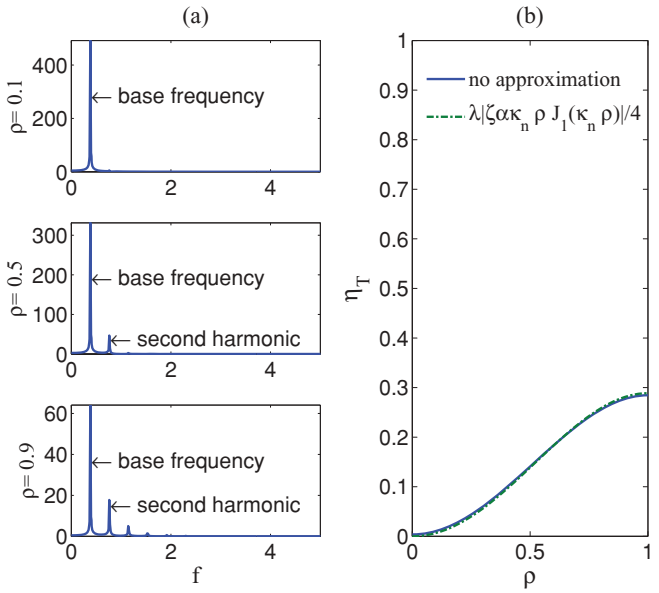

FIG. 3. (Color online) Results of calculations of cylindrical wave propagation in a nonlinear medium for the boundary-value problem $\mathcal{E}(1,\tau)=0$. (a) Frequency spectrum of the electric field in the $n=1$ mode. We use $\alpha=0.5$, $\zeta=1$, and $\varepsilon_1=2$. (b) Efficiencies of SHG η_T with different ρ, which ranges from 0 to 1.

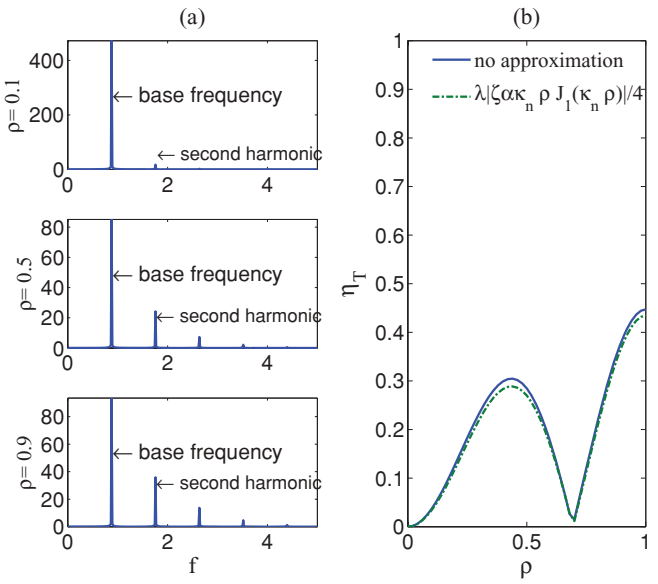

FIG. 4. (Color online) Results of calculations of cylindrical wave propagation in a nonlinear medium for the boundary-value problem $\mathcal{E}(1,\tau)=0$. (a) Frequency spectrum of the electric field in the $n=2$ mode. We use $\alpha=0.5$, $\zeta=1$, and $\varepsilon_1=2$. (b) Efficiencies of SHG η_T with different ρ, which ranges from 0 to 1.

Fig. 3(a) shows the frequency spectrum of the electric field at various ρ by using $\alpha=0.5$, $\zeta=1$, and $\varepsilon_1=2$. When $\rho=0.1$, there is hardly any second harmonic; when $\rho=0.5$, the second harmonic is pronounced; and when $\rho=0.9$, not only is the second harmonic but also the third harmonic is pronounced. Figure 3(b) shows the variation of η_T with ρ ranging from 0 to 1 calculated by different methods. The solid curve represents the results calculated directly using the exact solution in Eq. (14) and the dashed curve represents the results calculated using $\eta_T=\lambda|\zeta\alpha\kappa_n\rho J_1(\kappa_n\rho)|/4$. It is shown that η_T increases with ρ, as we have discussed, and $\eta_T=\lambda|\zeta\alpha\kappa_n\rho J_1(\kappa_n\rho)|/4$ fits well with the results calculated directly using the exact solution in Eq. (14) in the $n=1$ mode. To verify the higher mode, we calculate a spectrum analysis of the exact solution in Eq. (14) in the $n=2$ mode; the results are shown in Fig. 4. We can see that η_T is not increasing with ρ. Specifically, it has another extreme value at $\rho=\kappa_1/\kappa_2$ and another zero point at $\rho=\kappa_1^1/\kappa_2$, as we have discussed. Figure 4(b) shows that $\eta_T=\lambda|\zeta\alpha\kappa_n\rho J_1(\kappa_n\rho)|/4$ fits well with the results calculated directly using the exact solution in Eq. (14) in the $n=2$ mode. We can obtain similar results for the higher mode.

Our results are in agreement with those in Ref. [1] where it is shown that the nonlinear effects become more pronounced with increasing n and depend significantly on the coordinate ρ. It can be seen from Figs. 3 and 4 that the SHG of $n=2$ is more pronounced than the SHG of $n=1$ on the whole. However, it is violable at specific coordinates; for example, the SHG of $n=2$ is less pronounced than the SHG of $n=1$ for the case $\rho\approx 0.7$.

The problem of SHG under boundary-value conditions, which corresponds to the problem of SHG in a cavity, is an active research area in nonlinear optics. In these cases, electromagnetic waves are in the form of standing waves and several different phenomena are observed [20–24]. For most of this research, plane standing waves are considered. However, to the best of our knowledge, the features of SHG of cylindrical standing waves in a cylindrical cavity remain unknown. Thus the investigation of such a system has theoretical meaning. Petrov and Kudrin [1] have studied shock waves in a cylindrical cavity resonator filled with a nonlinear medium while in the present work we have analyzed the second-harmonic spectrum of the system. The results may be used in optical elements and geophysical prospecting, as suggested in Refs. [1,2].

III. COUPLED-WAVE EQUATIONS OF CYLINDRICAL ELECTROMAGNETIC WAVES INTERACTING WITH A NONLINEAR MEDIUM

A. Derivation of the coupled-wave equations in the cylindrical geometry

In this section we deduce coupled-wave equations of cylindrical electromagnetic waves interacting with a nonlinear medium. We also assume that the medium possesses an axis of symmetry, which is taken as the z axis of a cylindrical coordinate system (r,ϕ,z). If the fields are independent of ϕ and z, then the Maxwell equations can be written as [1]

$$\frac{\partial H}{\partial r}+\frac{H}{r}=\frac{\partial D}{\partial t},\quad \frac{\partial E}{\partial r}=\mu_0\frac{\partial H}{\partial t}, \tag{15}$$

where $H\equiv H_\phi(r,t)$, $E\equiv E_z(r,t)$, and $D(r,t)\equiv\epsilon_0 E+P$ with P being the intensity of the polarization of the medium. Hereinafter we will focus on electric fields to set up a classical theory that describes cylindrical electromagnetic wave propagation in a nonlinear medium.

For the case $P\propto E$, the medium is linear. Considering $D=\epsilon_0\varepsilon_1 E$, we can solve Eq. (15) by the method of variable separation. The solution is $E=AJ_0(kr)\exp(-i\varpi t)$. Now

considering the condition that $P = \epsilon_0\chi^{(1)}E + P_{\rm NL}$, on the basis of Eq. (15) we have

$$\frac{\partial^2 E}{\partial r^2} + \frac{1}{r}\frac{\partial E}{\partial r} = \frac{1}{v^2}\frac{\partial^2 E}{\partial t^2} + \mu_0\frac{\partial^2 P_{\rm NL}}{\partial t^2}, \tag{16}$$

where $1/v^2 = \epsilon_0\mu_0(1+\chi^{(1)}) = \epsilon_0\varepsilon_1\mu_0$. This equation is the fundamental equation of cylindrical nonlinear optics.

Following the example of plane waves [4–7], we present the electric field as

$$E = \frac{1}{2}\sum_i A_i J_0(k_i r)\exp(-i\varpi_i t) + A_i^* J_0(k_i r)\exp(i\varpi_i t) \tag{17}$$

and

$$P_{\rm NL} = \frac{1}{2}\sum_q P_q J_0(k_q r)\exp(-i\varpi_q t) + P_q^* J_0(k_q r)\exp(i\varpi_q t). \tag{18}$$

Also we can write $E = \frac{1}{2}\sum_i E(\varpi_i)$ and $P_{\rm NL} = \frac{1}{2}\sum_q P_{\rm NL}(\varpi_q)$, where $E(\varpi_i) = A_i J_0(k_i r)\exp(-i\varpi_i t)$, $E(-\varpi_i) = E^*(\varpi_i)$, $P_{\rm NL}(\varpi_q) = P_q J_0(k_q r)\exp(-i\varpi_q t)$, $P_{\rm NL}(-\varpi_q) = P_{\rm NL}^*(\varpi_q)$, and the summation runs over all frequencies including $\varpi > 0$ and $\varpi < 0$. Using these presentations we can simplify Eq. (16) and obtain the coupled-wave equations of cylindrical electromagnetic waves interacting with the nonlinear medium:

$$\frac{\partial^2 E(\varpi_i)}{\partial r^2} + \frac{1}{r}\frac{\partial E(\varpi_i)}{\partial r} + k_i^2 E(\varpi_i) = -\mu_0\varpi_i^2 P_{\rm NL}(\varpi_q = \varpi_i). \tag{19}$$

This equation describes cylindrical electromagnetic waves, coupled by $P_{\rm NL}$, with frequency ϖ_i propagating in a nonlinear medium. In what follows we will use this equation to study SHG.

We set $\varpi_1 = \varpi$ and $\varpi_2 = 2\varpi$. Using Eq. (19) we obtain

$$\begin{aligned}
&\frac{\partial^2 E(\varpi)}{\partial r^2} + \frac{1}{r}\frac{\partial E(\varpi)}{\partial r} + k^2 E(\varpi) \\
&\quad = -\mu_0\varpi^2 P_{\rm NL}(\varpi_q = \varpi), \\
&\frac{\partial^2 E(2\varpi)}{\partial r^2} + \frac{1}{r}\frac{\partial E(2\varpi)}{\partial r} + 4k^2 E(2\varpi) \\
&\quad = -4\mu_0\varpi^2 P_{\rm NL}(\varpi_q = 2\varpi),
\end{aligned} \tag{20}$$

where $P_{\rm NL}$ is used as the secondary nonlinear polarization $P^{(2)}$:

$$\begin{aligned}
P_{\rm NL}(\varpi_q = \varpi) &= \epsilon_0 2\chi(-\varpi, 2\varpi, -\varpi) : E(2\varpi)E^*(\varpi), \\
P_{\rm NL}(\varpi_q = 2\varpi) &= \epsilon_0\chi(-2\varpi, \varpi, \varpi) : E(\varpi)E(\varpi).
\end{aligned} \tag{21}$$

Using an effective nonlinear optical coefficient, we can rewrite Eq. (20) as

$$\begin{aligned}
&\frac{\partial^2 E(\varpi)}{\partial r^2} + \frac{1}{r}\frac{\partial E(\varpi)}{\partial r} + k^2 E(\varpi) \\
&\quad = -2\epsilon_0\mu_0\varpi^2 d_{\rm eff} E(2\varpi)E^*(\varpi), \\
&\frac{\partial^2 E(2\varpi)}{\partial r^2} + \frac{1}{r}\frac{\partial E(2\varpi)}{\partial r} + 4k^2 E(2\varpi) \\
&\quad = -4\epsilon_0\mu_0\varpi^2 d_{\rm eff} E^2(\varpi),
\end{aligned} \tag{22}$$

where $d_{\rm eff}$ is the effective nonlinear optical coefficient of the nonlinear medium, $E(\varpi) = A_1 J_0(kr)\exp(-i\varpi t)$, and $E(2\varpi) = A_2 J_0(2kr)\exp(-2i\varpi t)$. Then we have

$$\begin{aligned}
&\frac{\partial^2 A_1 J_0(kr)}{\partial r^2} + \frac{1}{r}\frac{\partial A_1 J_0(kr)}{\partial r} + k^2 A_1 J_0(kr) \\
&\quad = -2K A_1^* A_2 J_0(kr) J_0(2kr), \\
&\frac{\partial^2 A_2 J_0(2kr)}{\partial r^2} + \frac{1}{r}\frac{\partial A_2 J_0(2kr)}{\partial r} + 4k^2 A_2 J_0(2kr) \\
&\quad = -4K A_1^2 J_0^2(kr),
\end{aligned} \tag{23}$$

where $K = \epsilon_0\mu_0\varpi^2 d_{\rm eff}$. Simplifying Eq. (23) we obtain

$$\begin{aligned}
&\frac{\partial^2 A_1(r)}{\partial r^2} + \left(\frac{1}{r} - 2k\frac{J_1(kr)}{J_0(kr)}\right)\frac{\partial A_1(r)}{\partial r} = -2K A_1^* A_2 J_0(2kr), \\
&\frac{\partial^2 A_2(r)}{\partial r^2} + \left(\frac{1}{r} - 4k\frac{J_1(2kr)}{J_0(2kr)}\right)\frac{\partial A_2(r)}{\partial r} = -4K A_1^2\frac{J_0^2(kr)}{J_0(2kr)}.
\end{aligned} \tag{24}$$

By applying the slowly varying envelope approximation $\partial_r^2 A_i(r) \ll K A_i(r)$ and $\partial_r^2 A_i(r) \ll k\partial_r A_i(r)$, we can ignore $\partial_r^2 A_i(r)$ in Eq. (24) to obtain

$$\begin{aligned}
\frac{\partial A_1(r)}{\partial r} &= -2K J_0(2kr)\left(\frac{1}{r} - 2k\frac{J_1(kr)}{J_0(kr)}\right)^{-1} A_1^* A_2, \\
\frac{\partial A_2(r)}{\partial r} &= -4K\frac{J_0^2(kr)}{J_0(2kr)}\left(\frac{1}{r} - 4k\frac{J_1(2kr)}{J_0(2kr)}\right)^{-1} A_1^2.
\end{aligned} \tag{25}$$

On the basis of a small signal approximation, viz. $A_1(r) = A_1(0)$, we have

$$A_2(r) = 4K A_1^2(0)\int_0^r \frac{r J_0^2(kr)}{4k J_1(2kr) - J_0(2kr)}dr. \tag{26}$$

This expression can be used to calculate the amplitude of the second-harmonic generation when A_2 is small. If A_2 is not small enough, Eq. (26) is inapplicable. In this case, one can solve Eq. (25) numerically, which, however, is not recommended. A null point for $J_0(kr)$ and $J_0(2kr)$ will cause significant distortions because numerical calculation provides extreme sensitivity through a small range around the null point. Here we offer a method to deal with the problem. Returning to Eq. (23), we mark $A_1 J_0(kr)$ as $\tilde{A}_1$ and $A_2 J_0(2kr)$ as $\tilde{A}_2$. Then we have

$$\begin{aligned}
&\frac{\partial^2 \tilde{A}_1}{\partial r^2} + \frac{1}{r}\frac{\partial \tilde{A}_1}{\partial r} + k^2\tilde{A}_1 = -2K\tilde{A}_1^*\tilde{A}_2, \\
&\frac{\partial^2 \tilde{A}_2}{\partial r^2} + \frac{1}{r}\frac{\partial \tilde{A}_2}{\partial r} + 4k^2\tilde{A}_2 = -4K\tilde{A}_1^2.
\end{aligned} \tag{27}$$

Equation (27) can be solved numerically by considering A_1 and A_2 as functions of r, which gives the result of second-harmonic generation for the case that A_2 is not small enough. The light intensity can be calculated as $S_i = \varepsilon_0 cn\tilde{A}_i^2/2$ and the efficiency of the SHG is given by $\eta_s = S_2/S_1 = n(2\varpi)\tilde{A}_2^2/n(\varpi)\tilde{A}_1^2$ and $\eta_T = \tilde{A}_2/\tilde{A}_1$.

Figure 5 shows the results of calculations of cylindrical SHG based on coupled-wave equations. We use $\varpi = 6\times 10^8$ MHz and $\varepsilon_1 = 2$ (as in Fig. 2). Figure 5(a) shows $\tilde{A}_1$ and $\tilde{A}_2$ as functions of r for various $d_{\rm eff}$. For $S_2 \propto \tilde{A}_2^2$ and

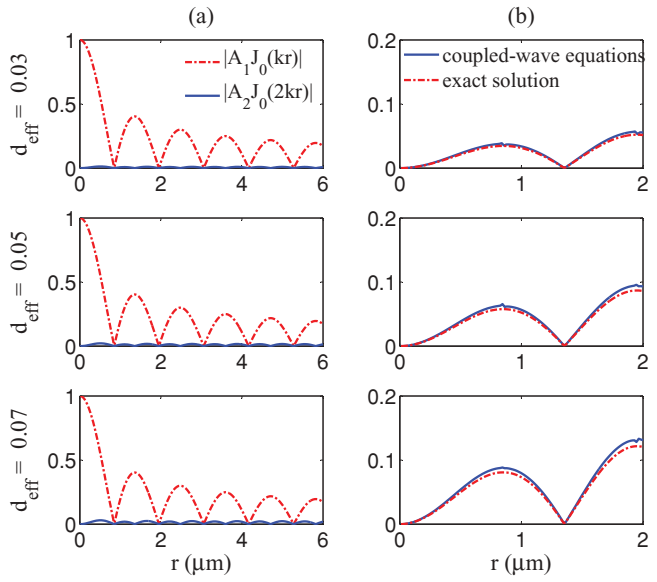

FIG. 5. (Color online) Results of SHG calculated using coupled-wave equations. We use $\varpi = 6 \times 10^8$ MHz and $\varepsilon_1 = 2$. (a) $\tilde{A}_1$ and $\tilde{A}_2$ as functions of r with various d_{eff}. (b) Efficiencies of second-harmonic η_T generation with different r, which ranges from 0 to 2 μm.

$\eta_s \propto \tilde{A}_2^2/\tilde{A}_1^2$, it is obvious that the light intensity of the second harmonic and the efficiency of SHG increase with the effective nonlinear optical coefficient d_{eff}, which is the same as for plane electromagnetic waves. However, the light intensity of the second harmonic and the efficiency of the SHG of cylindrical electromagnetic waves that vary with r are quite different from those of plane electromagnetic waves. For plane electromagnetic waves, the light intensity of the second harmonic and the efficiency of the SHG increase with r if there is phase matching [7]. For cylindrical electromagnetic waves, the light intensity of the second harmonic has fluctuations. Figure 5(b) shows the efficiency of second-harmonic η_T generation with different r, which ranges from 0 to 2 μm in the two methods. In Sec. II we obtained $\chi^{(2)} = \varepsilon_1\alpha/2$ and then $d_{\text{eff}} = \chi^{(2)}/2 = \alpha/2$ and $\eta_T = \lambda|\zeta d_{\text{eff}} kr J_1(kr)|/2$. From Fig. 5(b) we find that the descriptions of SHG by coupled-wave equations are in good agreement with the exact solution in Eq. (2).

B. Phase-matching condition of SHG in cylindrical nonlinear optics

An important issue with SHG is that of phase matching. In plane nonlinear optics [7], the phase-matching condition of SHG is $\Delta k = k(2\varpi) - 2k(\varpi) = 0$. We have the definition $k = \varpi\sqrt{\epsilon_0\varepsilon_1\mu_0}$. In our system $k(2\varpi) = 2\varpi\sqrt{\epsilon_0\varepsilon_1\mu_0}$ and $2k(\varpi) = 2\varpi\sqrt{\epsilon_0\varepsilon_1\mu_0}$. Obviously our system satisfies the phase-matching condition $\Delta k = 0$. However, the modulation of the SHG amplitude as well as the low conversion efficiency implies that there is no phase matching in this case. The facts suggest that the phase-matching condition of cylindrical nonlinear optics is different from that of plane nonlinear optics.

Now we consider the problem of the phase-matching condition of SHG in cylindrical nonlinear optics. We begin our discussion from Eqs. (25). For simplicity, we rewrite Eqs. (25) as

$$\frac{\partial A_1(r)}{\partial r} = -2K\psi_1 A_1^* A_2,$$
$$\frac{\partial A_2(r)}{\partial r} = -4K\psi_2 A_1^2, \tag{28}$$

where

$$\psi_1(r) = J_0(2kr)\left(\frac{1}{r} - 2k\frac{J_1(kr)}{J_0(kr)}\right)^{-1},$$
$$\psi_2(r) = \frac{J_0^2(kr)}{J_0(2kr)}\left(\frac{1}{r} - 4k\frac{J_1(2kr)}{J_0(2kr)}\right)^{-1}. \tag{29}$$

The functions ψ_1 and ψ_2 determine the phase-matching condition of the SHG. In plane nonlinear optics [7], $\psi_1 = \exp(i\Delta kr)$ and $\psi_2 = \exp(-i\Delta kr)$. In this case the phase-matching condition of the SHG is $\Delta k = k(2\varpi) - 2k(\varpi) = 0$ to ensure that ψ_1 and ψ_2 are positive. From Eqs. (29) we find that if the medium is homogeneous and nondispersive, then k is independent of r and ψ_1 and ψ_2 will not reach the phase-matching condition. This is the reason why the SHG amplitude is modulated and the conversion efficiency is low in our system.

Phase matching of the SHG in cylindrical nonlinear optics requires that the medium is inhomogeneous or dispersive, in which case one can discuss the condition of phase matching. A recent work [2] shows that the important technique suggested by Petrov and Kudrin [1] can be extended to inhomogeneous cases. So it is hopeful to use the exact solution to discuss phase matching of nonlinear optical phenomena. Our work shows that the inhomogeneity of the media will influence nonlinear optic effects and the mechanism is phase matching.

Here we provide a scheme of phase matching of SHG in cylindrical nonlinear optics for an inhomogeneous medium. The inhomogeneity of the media can be described as $\varepsilon(r) \propto r^{-2}$, viz. $k \propto r^{-1}$; thus we have $\psi_1 \propto r$ and $\psi_2 \propto r$, which ensure that ψ_1 and ψ_2 are large and positive for any r. Figure 6 shows the results of SHG calculated using coupled-wave equations for such cases. We can find that the modulations of the SHG amplitude have disappeared and the conversion efficiency is much larger than for the homogeneous cases. This type of space-variant polarizability [r^β or $(r-a)^\beta$] has been used in many works [2,25–29]. For example, Jiang *et al.* [29] used $\varepsilon_\phi = kr$ and $\varepsilon_r = 1/kr$ to bend electromagnetic waves and showed that the inhomogenous factor is realizable. The effect of SHG strongly depends on the inhomogeneity of the media, which may be used in a noninvasive, noncontact probe of the nonlinear medium, such as a defect of crystals [2,6,7].

IV. DISCUSSION

It is worth mentioning the differences between our system and the conical wave propagation, which is an active research area in nonlinear optics [15–19]. While at first sight there are certain similarities between our system and the conical wave propagation, there are in fact essential differences between them. In our system the emission of the second harmonic is parallel to the fundamental wave. Similarly, we can also show that our work is not a special case of the conical wave

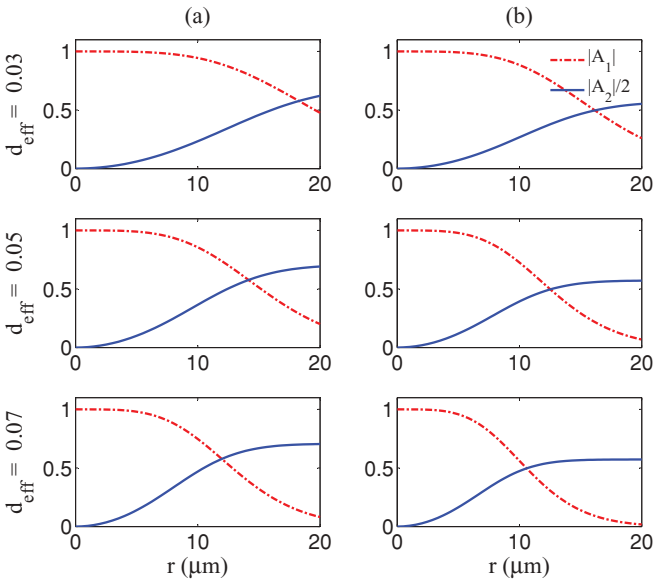

FIG. 6. (Color online) Results of SHG calculated using coupled-wave equations for an inhomogeneous medium. $|A_1|$ and $|A_1|/2$ as functions of r for various d_{eff} are shown for $k(r) = q/r$, where q is a constant. We use $\varpi = 6 \times 10^8$ MHz, $\varepsilon_1 = 2$, and (a) $q = 4.6$ and (b) $q = 10$.

propagation. The important difference is that in those cases (see, e.g., Ref. [19]) the phase-matching condition is $\mathbf{k}_2 - 2\mathbf{k}_1 = \mathbf{G}_m$, while in our system it is not. The amplitude of the second-harmonic field is given by

$$E^{2\varpi}(\rho,z) = 2\pi S(z)\exp(-ik_{2z}z)[iJ_1(k_2\rho\sin\alpha)\mathbf{u}_\rho - \tan\alpha J_0(k_2\rho\sin\alpha)\mathbf{u}_z] \quad (30)$$

in the conical wave propagation case; in our case the amplitude of the second-harmonic field takes the form

$$E^{2\varpi} \approx -\alpha\zeta^2 kr J_1(kr)J_0(kr)/2. \quad (31)$$

So the mechanism, phase-matching condition, and amplitude of the second-harmonic field are all different from the system of the conical wave propagation.

Our analysis in current geometry includes two different systems: a cylindrical traveling wave and a cylindrical standing wave. The former means that the cylindrical wave propagates in an infinite medium, while the latter means that the system is under boundary-value conditions. Both systems can be produced by experiment, especially the cylindrical SHG under boundary-value conditions, which has been proposed in Ref. [1]. The experimental setup uses a cylindrical cavity resonator of radius a and height L, which is a perfectly conducting circular cylinder. The cavity resonator is filled with a nonlinear medium. In this case one can excite $E_{0n0}(TM_{0n0})$ modes and the nonlinear phenomena can be observed by using a probe fixed in the cavity. For more details one can refer to the original literature [1].

There are several possible experimental setups of cylindrical SHG without boundary-value conditions. Here we use a slit source to obtain cylindrical waves, which is frequently used in practice [30]. A schematic of a possible experimental setup is shown in Fig. 7. The nonlinear medium (shown in green in Fig. 7) of a semicylinder is used and the cut surface is opaque

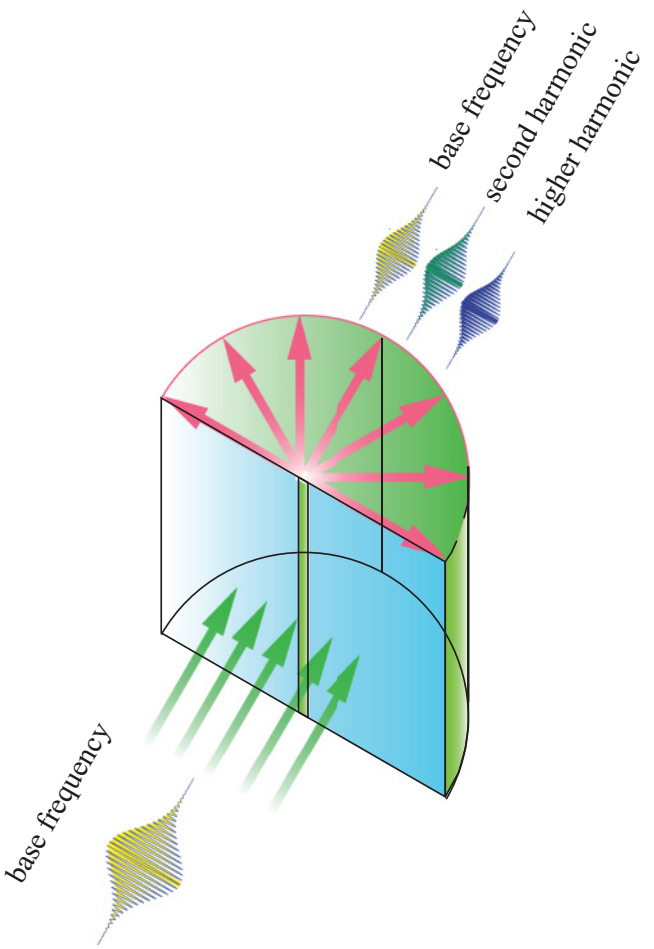

FIG. 7. (Color online) Schematic of the experimental setup. The nonlinear medium (green) of a semicylinder is used and the cut surface is opaque (blue) except for the axis of the semicylinder, which can form a slit and produce cylindrical waves. When a beam of light with base frequency is incident upon the slit, cylindrical waves propagate in the nonlinear medium and second- and higher-harmonic generation will occur. Using a detector fixed around the medium, one can observe cylindrical SHG.

(shown in blue in Fig. 7) except for the axis of the semicylinder, which can form a slit and produce cylindrical waves. When a beam of light with base frequency is incident upon the slit, there are cylindrical waves propagating in the nonlinear medium and second- and higher-harmonic generation will occur. Using a detector fixed around the medium, one can observe the cylindrical SHG.

Propagation of cylindrical and spherical waves in nonlinear media is of great interest in theory and for application; however, it remains poorly studied. In a recent work [1] an exact solution that describes the propagation of cylindrical electromagnetic waves in a nonlinear nondispersive medium was obtained and used to discuss electromagnetic shock waves. The exact solution is of great importance and in the present article we show that it can be used to discuss not only electromagnetic shock waves, but also SHG. Figure 5(b) shows that the exact solution in Eq. (2) can be used to deal with the SHG very well. Furthermore, it has advantages in several aspects, such as dealing with problems of SHG under initial-value and

boundary-value conditions, which are complicated by using coupled-wave equations. Moreover, a recent work [2] shows that this important technique can be extended to deal with problems of cylindrical electromagnetic wave propagation in an inhomogeneous nonlinear and nondispersive medium. So it is hopeful to use the exact solution to discuss nonlinear optical phenomena in an inhomogeneous medium, which is also an extremely complicated problem. In contrast, although the exact solution has great success in dealing with the SHG, the coupled-wave equations of cylindrical electromagnetic waves interacting with a nonlinear medium are also necessary. The coupled-wave equations can be directly associated with the dispersion of media and can be extended to deal with problems of sum frequency, four-wave mixing, and so on.

V. CONCLUSION

We have used two methods to deal with the problem of cylindrical SHG. One method uses the exact solution obtained recently. We have exported the exact solution and found a simple method to deduce the SHG from it. The other method uses the traditional coupled-wave equations. We have set up coupled-wave equations of cylindrical electromagnetic waves interacting with a nonlinear medium to describe SHG. Using the coupled-wave equations, we have analyzed features of cylindrical SHG and found that the results are in good agreement with those obtained by using the exact solution. Our results show that both methods are useful in dealing with the problem of cylindrical SHG and each of them has advantages in some aspects.

ACKNOWLEDGMENTS

The work was supported in part by the National Science Foundation of China (Grants No. 10874050, No. 10975054, No. 91021011, No. 11005057, and No. 10634060), the National Fundamental Research Program of China (Grant No. 2005CB724508), the Science Innovation Foundation of the Huazhong University of Science and Technology grant, and the Research Fund for the Doctoral Program of Higher Education of China (Grant No. 200804870051). H.X., L.-G.S., and J.F.G. were also supported in part by the Program for Excellent Doctoral Students granted by the Ministry of Education China. The authors acknowledge Professor Ying Wu for his enlightening suggestions and the anonymous referee for insightful comments.

[1] E. Y. Petrov and A. V. Kudrin, Phys. Rev. Lett. **104**, 190404 (2010).
[2] H. Xiong, L.-G. Si, P. Huang, and X. Yang, Phys. Rev. E **82**, 057602 (2010).
[3] P. A. Franken, A. E. Hill, C. W. Peters, and G. Weinreich, Phys. Rev. Lett. **7**, 118 (1961).
[4] J. A. Armstrong, N. Bloembergen, J. Ducuing, and P. S. Pershan, Phys. Rev. **127**, 1918 (1962).
[5] N. Bloembergen and P. S. Pershan, Phys. Rev. **128**, 606 (1962).
[6] N. Bloembergen, Rev. Mod. Phys. **54**, 685 (1982).
[7] Y. R. Shen, *Principles of Nonlinear Optics* (Wiley, New York, 1984).
[8] Y. Zeng, W. Hoyer, J. Liu, S. W. Koch, and J. V. Moloney, Phys. Rev. B **79**, 235109 (2009).
[9] S. A. Yang, X. Li, A. D. Bristow, and J. E. Sipe, Phys. Rev. B **80**, 165306 (2009).
[10] R. A. Ganeev, H. Singhal, P. A. Naik, J. A. Chakera, H. S. Vora, R. A. Khan, and P. D. Gupta, Phys. Rev. A **82**, 053831 (2010).
[11] T. Auguste, O. Gobert, and B. Carré, Phys. Rev. A **78**, 033411 (2008).
[12] C. C. Chirilă and M. Lein, Phys. Rev. A **77**, 043403 (2008).
[13] H. Hu and J. Yuan, Phys. Rev. A **78**, 063826 (2008).
[14] P. Hewageegana and V. Apalkov, Phys. Rev. B **77**, 075132 (2008).
[15] S. M. Saltiel, D. N. Neshev, R. Fischer, W. Krolikowski, A. Arie, and Y. S. Kivshar, Opt. Lett. **33**, 527 (2008).
[16] N. Voloch, T. Ellenbogen, and A. Arie, J. Opt. Soc. Am. B **26**, 42 (2009).
[17] S. M. Saltiel, D. N. Neshev, R. Fischer, W. Krolikowski, A. Arie, and Y. S. Kivshar, Phys. Rev. Lett. **100**, 103902 (2008).
[18] S. M. Saltiel, D. N. Neshev, R. Fischer, W. Krolikowski, A. Arie, and Y. S. Kivshar, Jpn. J. Appl. Phys. **47**, 6777 (2008).
[19] S. Saltiel, W. Krolikowski, D. Neshev, and Y. S. Kivshar, Opt. Express **15**, 4132 (2007).
[20] H.-B. Lin and A. J. Campillo, Phys. Rev. Lett. **73**, 2440 (1994).
[21] K. Koch and G. T. Moore, J. Opt. Soc. Am. B **16**, 448 (1999).
[22] V. S. Ilchenko, A. A. Savchenkov, A. B. Matsko, and L. Maleki, Phys. Rev. Lett. **92**, 043903 (2004).
[23] A. Vukics, W. Niedenzu, and H. Ritsch, Phys. Rev. A **79**, 013828 (2009).
[24] R. Krischek, W. Wieczorek, A. Ozawa, N. Kiesel, P. Michelberger, T. Udem, and H. Weinfurter, Nature Photon. **4**, 170 (2010).
[25] Z. Ruan, M. Yan, C. W. Neff, and M. Qiu, Phys. Rev. Lett. **99**, 113903 (2007).
[26] M. Yan, Z. Ruan, and M. Qiu, Phys. Rev. Lett. **99**, 233901 (2007).
[27] Y. Lai, H. Chen, Z. Q. Zhang, and C. T. Chan, Phys. Rev. Lett. **102**, 093901 (2009).
[28] Y. You, G. W. Kattawar, and P. Yang, Opt. Express **17**, 6591 (2009).
[29] W. X. Jiang, T. J. Cui, X. Y. Zhou, X. M. Yang, and Q. Cheng, Phys. Rev. E **78**, 066607 (2008).
[30] M. Bass, *Handbook of Optics*, 3rd ed. (McGraw-Hill, New York, 2010).